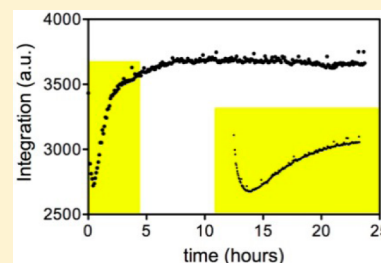


Solvent Isotope-Induced Equilibrium Perturbation for Isocitrate Lyase

Christine E. Quartararo, Timin Hadi, Sean M. Cahill, and John S. Blanchard*

Department of Biochemistry, Albert Einstein College of Medicine, 1300 Morris Park Avenue, Bronx, New York 10461, United States

ABSTRACT: Isocitrate lyase (ICL) catalyzes the reversible retro-aldol cleavage of isocitrate to generate glyoxylate and succinate. ICL is the first enzyme of the glyoxylate shunt, which allows for the anaplerosis of citric acid cycle intermediates under nutrient limiting conditions. In *Mycobacterium tuberculosis*, the source of ICL for these studies, ICL is vital for the persistence phase of the bacterium's life cycle. Solvent kinetic isotope effects (KIEs) in the direction of isocitrate cleavage ($D_2O V = 2.0 \pm 0.1$, and $D_2O [V/K_{isocitrate}] = 2.2 \pm 0.3$) arise from the initial deprotonation of the C2 hydroxyl group of isocitrate or the protonation of the aci-acid of the succinate product of the isocitrate aldol cleavage by a solvent-derived proton. This KIE suggested that an equilibrium mixture of all protiated isocitrate, glyoxylate, and succinate prepared in D_2O would undergo transient changes in equilibrium concentrations as a result of the solvent KIE and solvent-derived deuterium incorporation into both succinate and isocitrate. No change in the isotopic composition of glyoxylate was expected or observed. We have directly monitored the changing concentrations of all isotopic species of all reactants and products using a combination of nuclear magnetic resonance (NMR) spectroscopy and mass spectrometry. Continuous monitoring of glyoxylate by 1H NMR spectroscopy shows a clear equilibrium perturbation in D_2O . The final equilibrium isotopic composition of reactants in D_2O revealed dideuterated succinate, protiated glyoxylate, and monodeuterated isocitrate, with the transient appearance and disappearance of monodeuterated succinate. A model for the equilibrium perturbation of substrate species and their time-dependent isotopic composition is presented.



Isocitrate lyase (ICL) is present in a number of bacteria, fungi, and plants, but not in humans.¹ The retro-aldol cleavage of isocitrate to succinate and glyoxylate catalyzed by ICL is the first step of the glyoxylate shunt, a two-enzyme pathway that converts AcCoA and isocitrate into the four-carbon citric acid cycle intermediates succinate and malate. These steps bypass the isocitrate and α -ketoglutarate dehydrogenase steps of the citric acid cycle, preventing the loss of the two carbon units of acetyl-coenzyme A (AcCoA) from being released as CO_2 and allowing for the incorporation of the two carbon units, via gluconeogenesis, into triose and hexose pools. *Mycobacterium tuberculosis* requires ICL to maintain metabolite pools when the bacterium is restricted to oxidation of fatty acids as a food source during the persistence phase of the bacterial life cycle. The persistence phase is particularly difficult to treat, and a knockout of ICL in *M. tuberculosis* has shown attenuated virulence in mice.²

The original identification of the enzyme activity of ICL was reported in 1953³ and was followed by a series of reports that demonstrated that *threo*- D_5 -isocitrate was the true substrate and the enzyme was induced when organisms were grown on acetate.^{4–6} Studies of the stereochemistry of the reaction revealed that cleavage of isocitrate in D_2O yielded $[2-^2H]$ -L-succinate as the product, a net inversion of configuration, and was associated with a small solvent kinetic isotope effect of ~ 1.2 .^{7,8} In these studies, it was demonstrated that the incorporation of solvent-derived deuterium into succinate was absolutely dependent upon glyoxylate being present, suggesting that glyoxylate bound to the active site metal, followed by

succinate. Crystal structures of the *M. tuberculosis* ICL in which the active site magnesium ion is coordinated by the aldehyde and carboxylate of glyoxylate and nitropropionate, an isosteric mimic of the carbanion of succinate, support this interpretation.⁹

Solvent isotopic composition can influence both the rates of enzyme-catalyzed reactions (solvent kinetic isotope effects) and, in the case of solvent-derived deuterium incorporation into nonexchangeable C–H bonds in products, solvent equilibrium isotope effects. The former reveal potential rate-limiting proton transfer steps in the chemical reaction, while the latter reflect the stiffness of the C–H bond in the deuterated product compared to water. These two effects are not mutually exclusive, and one of the first reports suggesting such coupling was reported by Cardinale and Abeles for proline racemase. By monitoring the racemization of L- to D-proline by optical rotation, they found that the reaction in D_2O approached and “overshot” the equilibrium concentrations of the reactants and then returned to equilibrium. This is in contrast to the reaction in H_2O , which approached equilibrium concentrations but never overshoot them. The authors proposed that this was due to the incorporation of deuterium from solvent into the $[\alpha\text{-}^2H]$ -D-proline product and the slower reversion of D- to L-proline as a result of a solvent kinetic isotope effect.¹⁰ Subsequently, Schimerlik et al. demonstrated that when an

Received: September 26, 2013

Revised: November 18, 2013

Published: November 21, 2013



equilibrium mixture of enzyme substrates was prepared with hydrogen-containing substrates and deuterium-containing products, and enzyme was added, a transient perturbation of the concentrations of substrates and products was observed because of the KIEs, and the magnitude of the KIE could be determined from the magnitude of the displacement, or isotopically induced “perturbation”.¹¹ This method was sensitive enough to measure heavy atom KIEs, and in the original report, ²H-, ¹³C-, and ¹⁵N-substituted substrates were used to determine primary KIEs on malate dehydrogenase, malic enzyme, and glutamate dehydrogenase.¹¹

In a case more related to this report, primary and secondary deuterium, solvent deuterium, and ¹⁸O kinetic and equilibrium isotope effects were reported for pig heart fumarase.¹² Solvent-derived deuterium is incorporated into the C3–H_R bond of (2S)-malate, and the measured primary solvent kinetic and equilibrium isotope effects were inverse (0.92 and 0.98, respectively). The latter equilibrium isotope effect is likely to be similar to the effect for the incorporation of solvent deuterium into succinate (and isocitrate) in the ICL reaction.

All of the examples mentioned above relied on the continuous measurement of changes in absorbance or optical rotary dispersion. Our initial attempts to measure the ICL reaction and potential perturbation using optical rotary dispersion due to changes in the concentration of (2R,3S)-isocitrate revealed that this method would not be sufficiently sensitive for the performance of the desired experiments. Rather, we posited that ¹H nuclear magnetic resonance (NMR) spectroscopy and small molecule mass spectrometry could be used to semicontinuously measure both the concentrations and isotopic composition of all substrates and products simultaneously.

MATERIALS AND METHODS

Materials. All kinetic experiments used isocitrate from Sigma-Aldrich as the DL-isocitric acid trisodium salt hydrate. All mass spectrometry, NMR spectroscopy, and *K*_{eq} experiments used (2R,3S)-isocitrate enzymatically synthesized with ICL and purified as described previously.¹³ In both cases, the concentration of isocitrate was determined enzymatically with isocitrate dehydrogenase.

Cloning, Expression, and Purification. *M. tuberculosis* *icl1* (Rv0467) was amplified via polymerase chain reaction (PCR) from H37Rv *M. tuberculosis* DNA with NdeI and HindIII restriction sites. The PCR product was ligated into a pET-28a(+) vector, containing an N-terminal His₆ tag. After positive sequencing results had been recorded, the plasmid was transformed into T7 express competent *Escherichia coli*. A single colony was used to generate a starter culture, of which 10 mL was added to each of six 2 L flasks containing 1 L of Luria broth and 30 μg/mL kanamycin. The *E. coli* cells were grown, while being shaken at 200 rpm at 37 °C, until *A*₆₀₀ reached 0.6. After the samples had been cooled, 0.5 mM IPTG was added to each flask. The *E. coli* continued to grow, while being shaken, overnight at 18 °C. Cells were collected by centrifugation and resuspended in 50 mM Tris (pH 8.0) containing 250 mM NaCl, 1 mM imidazole, one tablet of EDTA-free protease inhibitor cocktail, 800 units of DNase, and 10 mg of lysozyme. After 30 min, cells were lysed by sonication, and cellular debris were removed by centrifugation. Batch nickel affinity purification was performed using 1 mL of Ni-NTA resin slurry for every 4 mL of lysate. After a 1 h incubation, the slurry mixture was poured into a column, and elution was performed

stepwise with a gradient from 0 to 500 mM imidazole. ICL-containing fractions were dialyzed into a storage buffer that consisted of 50 mM HEPES (pH 7.0) containing 150 mM NaCl and 50% glycerol and stored at –20 °C. The protein concentration was determined by the absorbance with an ϵ of 71975 M^{–1}.¹⁴

Measurement of ICL Activity. Isocitrate cleavage was monitored by coupling glyoxylate formation to lactate dehydrogenase (LDH), which can convert glyoxylate to glycolate with the concomitant oxidation of NADH. A typical 1 mL assay contained 50 mM HEPES (pH 7.5) containing 5 mM MgCl₂, 50 μM NADH, 25 units of LDH, and varying amounts of isocitrate. The reaction was initiated with 20 nM ICL, from an intermediate dilution in 50 mM HEPES (pH 7.5) containing 150 mM NaCl, 5 mM MgCl₂, and 5 mg/mL BSA. In the opposite direction, isocitrate formation was coupled to isocitrate dehydrogenase, which catalyzes the reduction of NADP⁺ with conversion of isocitrate to α -ketoglutarate. A typical 1 mL assay contained 50 mM HEPES (pH 7.5) containing 5 mM MgCl₂, 5 mM MnCl₂, 500 μM NADP⁺, 5 mM (saturating) glyoxylate, 80 nM *M. tuberculosis* ICDH-1, and varying amounts of succinate or [2,2,3,3-²H]succinate. The reactions were initiated with 20 nM ICL from the same intermediate dilution as the cleavage reactions.

Steady-State Data Analysis. Initial kinetic parameters were obtained by fitting to the Michaelis–Menten equation. Primary KIEs and solvent KIEs were fit to eq 1

$$v = VS/[K(1 + F_i E_{V/K}) + S(1 + F_i E_V)] \quad (1)$$

where *F*_i = 0 or 1 in the primary KIE experiment and *F*_i = 0 or 0.945 in the solvent KIE experiment.

***K*_{eq} Determination.** *K*_{eq} was determined by starting a reaction in 50 mM HEPES (pH 7.5) containing 5 mM MgCl₂, 480 μM isocitrate, and 1.5 μM ICL. The reaction was determined to reach equilibrium when the amount of glyoxylate was no longer changing, as judged by the LDH-coupled assay. A *K*_{eq} of 0.00107 ± 0.00004 M was determined to estimate equilibrium concentrations of the substrates and products in the ICL reaction. *K*_{eq} is reported in the direction of isocitrate cleavage and was determined in triplicate.^a

NMR Equilibrium Perturbation Experiments. The determined equilibrium concentrations of substrates from the *K*_{eq} determination experiments were scaled up 30-fold in 50 mM sodium phosphate buffer or 50 mM ammonium acetate buffer (pH 7.5) (3.9 mM isocitrate, 10.5 mM succinate, and 10.5 mM glyoxylate). ICL, which had been exchanged into the appropriate buffer, was then added and left in H₂O for 48 h, to ensure exact equilibrium conditions. ICL was removed with a 10K molecular weight cutoff Amicon filter, and the mixture was frozen and lyophilized prior to reconstitution in deuterated solvent. Because ammonium acetate is volatile, 50 mM deuterated ammonium acetate buffer (pD 7.8) was used to reconstitute the mixture after lyophilization, while D₂O was used for the sodium phosphate-buffered experiments. All of the ¹H NMR spectra for equilibrium perturbation experiments were recorded at 25 °C on a Bruker DRX 600 MHz spectrometer, and one-dimensional proton spectra were recorded using 64 scans with a pulse width of 30°, a sweep width of 20 ppm sampled with 64K points, and a recycle delay of 2 s for a total of ~5 min per spectrum. All spectra were processed with a –0.20 Hz exponential window function. For each experiment, 600 μL of the reconstituted equilibrium mixture was transferred to a NMR tube and a spectrum was acquired. ICL, exchanged into

the appropriate deuterated buffer, was then added to the reaction mixture (final concentration of 0.3, 1, or 5 μM) and the solution mixed thoroughly. NMR spectra of the ICL-containing equilibrium mixture were recorded continuously until the reaction was deemed to have reached equilibrium. NMR spectra were analyzed using MestReNova. For initial identification of the deuterated species present in the mixture, an aliquot of an in-progress NMR equilibrium perturbation experiment (0.3 μM ICL) was diluted into methanol and centrifuged to remove precipitated enzyme. The sample was analyzed in negative mode by mass spectrometry using a 12 T Fourier transform ion cyclotron resonance mass spectrometer (Agilent).

Mass Spectrometry Time Course Experiment. For mass spectrometry experiments, an equilibrium mixture in ammonium acetate buffer was prepared in a manner identical to that described above for NMR spectroscopy experiments. After reconstitution of the lyophilized mixture in 50 mM deuterated ammonium acetate buffer (pD 7.0), ICL was added (final concentration of 1 μM) to initiate the reaction. Individual time points were taken by quenching samples of the reaction mixture in methanol in a 1:100 dilution. The methanol used as the quenching agent contained 103.95 μM malate as an internal standard. Samples were centrifuged to remove precipitated ICL and transferred to vials for mass spectrometry analysis. Time course mass spectrometry was performed in negative mode on a Waters Synapt G2 ESI mass spectrometer, and all data were processed using MassLynx and TargetLynx (Waters). For each time point, three replicate measurements were obtained and each of the metabolites of interest was quantified. Using malate as the internal standard, the peak area of each compound was obtained.

Graphing and Fitting. Graphing and fitting were performed with GraphPad Prism version 5.0d. The error bars are the standard deviations of duplicate or triplicate measurements, and the error reported with the fitted values is the error of the fit. A.u. is an abbreviation for arbitrary units.

RESULTS AND DISCUSSION

Steady-State Kinetics. Initial kinetic parameters were determined by fitting the data to the Michaelis–Menten equation. In the direction of isocitrate cleavage, $k_{\text{cat}} = 5.2 \pm 0.2 \text{ s}^{-1}$ and $K_{\text{isocitrate}} = 45 \pm 7 \mu\text{M}$. In the direction of isocitrate formation, $k_{\text{cat}} = 3.6 \pm 0.2 \text{ s}^{-1}$, $K_{\text{glyoxylate}} = 400 \pm 70 \mu\text{M}$, and $K_{\text{succinate}} = 240 \pm 40 \mu\text{M}$. Solvent KIEs on isocitrate cleavage of 2.0 ± 0.1 ($^{2}\text{D}_2\text{O}$) and 2.2 ± 0.3 ($^{2}\text{D}_2\text{O}[V/K_{\text{isocitrate}}]$) were observed (Figure 1A). A small viscosity effect was detected when the reaction mixture in water was compared to a glycerol control [8.5% (w/v)] of the same viscosity as D_2O , and the solvent KIEs were calculated in comparison to the glycerol control. The observation of a solvent KIE could indicate that initiation of the isocitrate cleavage reaction by the removal of a proton from the C2 hydroxyl group of isocitrate is partially rate-limiting or that the protonation of the succinate carbanion by a solvent-derived proton from Cys191 is partially rate-limiting (see below).¹⁵ If the removal of a proton from the C2 hydroxyl is rate-limiting, this would suggest that in the reverse reaction that alkoxide protonation would be more energetically difficult than the C–C bond-forming reaction, which is unlikely. Intimate metal chelation could stabilize the alkoxide in the condensation reaction but would likely destabilize the alcohol in the isocitrate cleavage reaction. Consistent with the idea that protonation of the succinate anion is the source of the

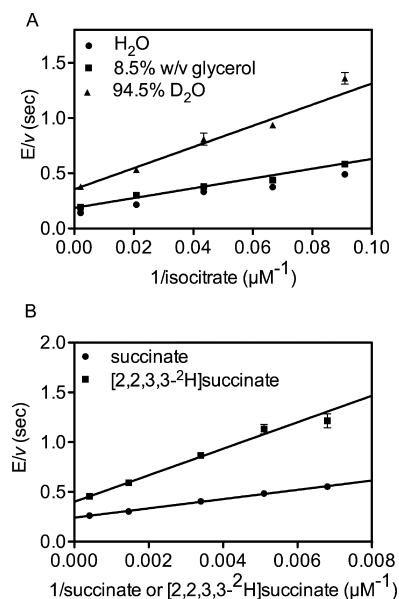
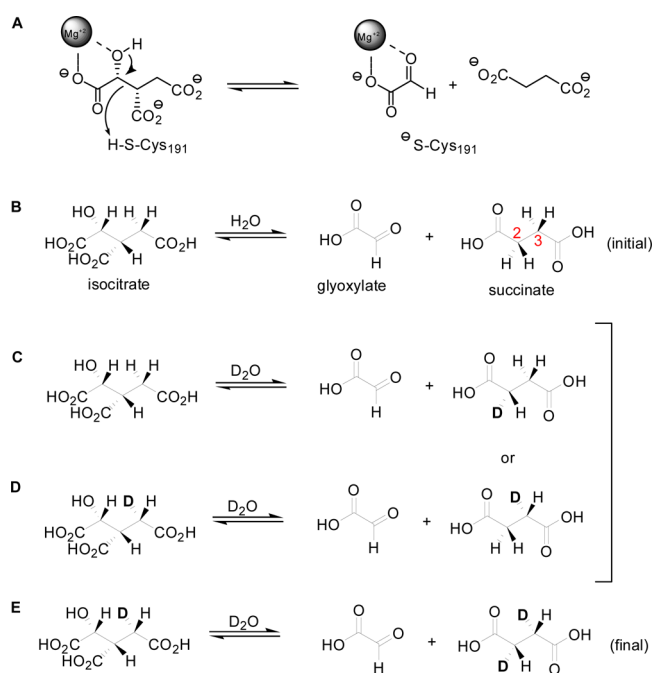


Figure 1. (A) Solvent kinetic isotope effect in comparison to glycerol control. $^{2}\text{D}_2\text{O}V = 2.0 \pm 0.1$, and $^{2}\text{D}_2\text{O}[V/K_{\text{isocitrate}}] = 2.2 \pm 0.3$. (B) Primary kinetic isotope effect. $^{2}\text{D}V = 1.7 \pm 0.1$, and $^{2}\text{D}V/K_{\text{succinate}} = 2.9 \pm 0.2$.

solvent kinetic isotope effect and the rate-limiting step, a large primary kinetic isotope effect is observed when the formation of isocitrate is compared to the formation of isocitrate from tetradeuterosuccinate [$^{2}\text{D}V = 1.7 \pm 0.1$, and $^{2}\text{D}V/K_{\text{succinate}} = 2.9 \pm 0.2$ (Figure 1B)]. This is also supported by studies reported by Moynihan and Murkin.¹⁵

It was therefore necessary to account for the incorporation of solvent-derived deuterium into the reactants. As shown in Scheme 1, the species in panel B represent the isotopic

Scheme 1. Chemical Mechanism (A) and Distribution of Isotopologues before (B), during (C and D), and after (E) Incubation with D_2O



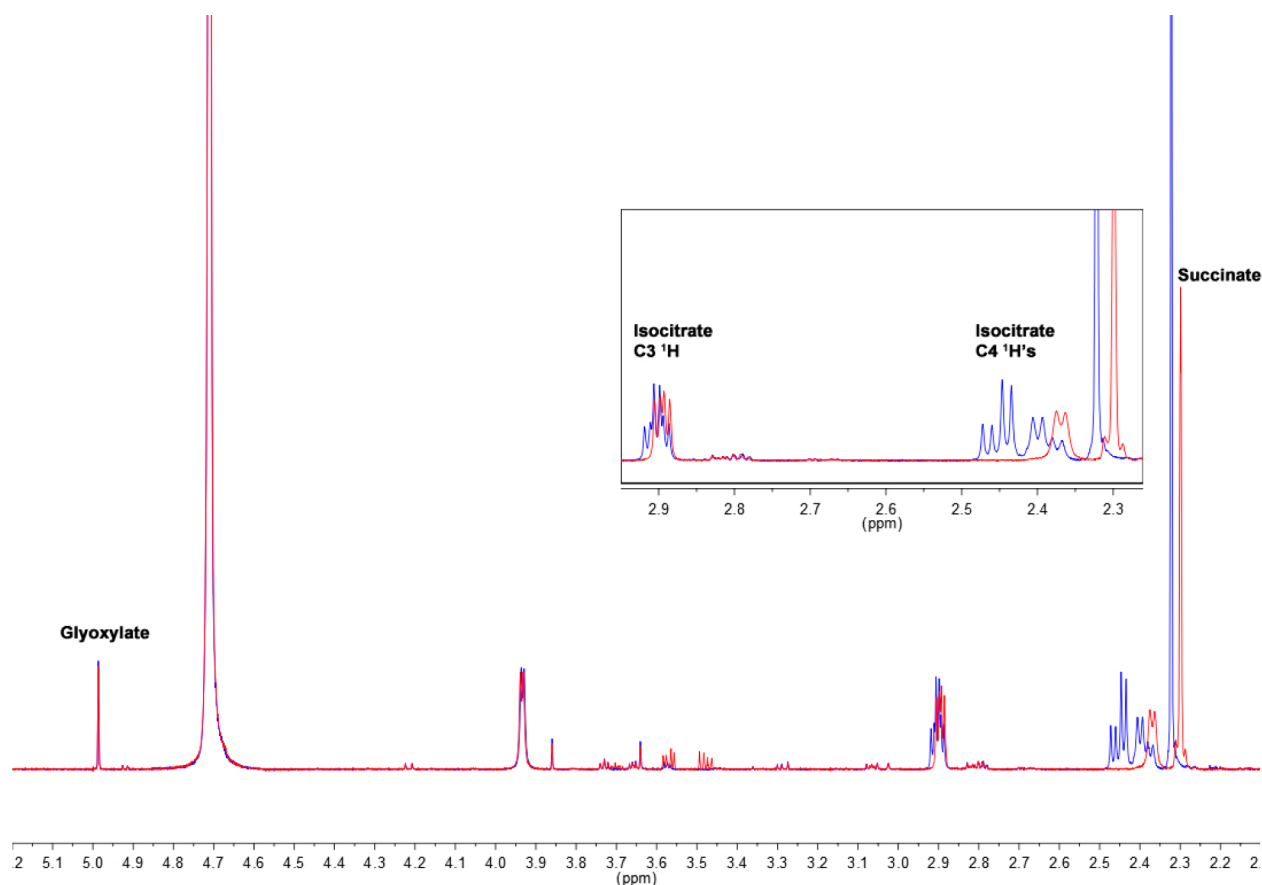


Figure 2. NMR spectra before and after the addition of ICL. Before ICL addition (blue spectrum) and 23.6 h after the addition of 5 μ M ICL, when isotopic equilibrium has been reached (red spectrum).

composition of the reactants at equilibrium in H_2O . When the mixture is reconstituted in D_2O and ICL is added, the isocitrate cleavage reaction yields a succinate molecule with a solvent-derived deuterium at the C2 position (Scheme 1C). Because succinate is symmetric, the monodeuterated molecule can enter the active site in two different orientations, allowing chemistry to occur by cleavage of the C–D bond (Scheme 1C) or cleavage of the C–H bond (Scheme 1D), generating fully protiated isocitrate or isocitrate bearing a deuterium at C4. The ratio of the two reaction fluxes will be subject to a substantial intramolecular isotope effect due to the large primary $^{\text{D}}V/K_{\text{succinate}}$ of 2.9 ± 0.2 observed in the condensation direction. Finally, cleavage of $[4\text{-}^2\text{H}]\text{isocitrate}$ in D_2O would yield dideuterated succinate $[[2,3\text{-}^2\text{H}_2]\text{-threo-}L\text{-succinate}$ (Scheme 1E)].

Isotopic Changes in Reactants Caused by D_2O . An initial comparison of the ^1H NMR spectra before and after the addition of ICL indicated that the incorporation of deuterium into isocitrate and succinate had occurred (Figure 2). The initial mixture in D_2O , before the addition of ICL, is representative of the equilibrium compositions and concentrations of substrates and products in H_2O (blue spectrum, Figure 2). After the addition of ICL and incubation of the mixture at room temperature, a new equilibrium in D_2O is reached (red spectrum, Figure 2). The two doublets of doublets in the region of the ^1H NMR spectrum between 2.48 and 2.34 ppm collapse to a single doublet that is shifted slightly upfield after incubation with ICL (final concentration of 5 μM). This can be attributed to the stereospecific incorporation of a

deuterium atom at the C4 position of isocitrate. The reduced complexity of the peak at 2.90 ppm corresponding to the C3 hydrogen of isocitrate is also consistent with the incorporation of a deuterium at C4. Incorporation of deuterium into succinate also occurs enzymatically during the ICL-catalyzed reaction. The peak at 2.32 ppm due to the succinate hydrogens undergoes an upfield shift and a decrease in area corresponding to the loss of two hydrogens after incubation with the enzyme. This result explains the previous report that 1.4 deuterium atoms were found in succinate isolated from the cleavage of isocitrate by the enzyme in D_2O , suggesting that in this experiment, isotopic equilibrium had not been achieved.⁸

Equilibrium Perturbation. As revealed above, there is no exchange of solvent into glyoxylate, suggesting that this reactant would be ideal for monitoring the potential solvent deuterium-induced equilibrium perturbation. The glyoxylate hydrate $[K_{\text{eq(hydrate/aldehyde)}} = 163]^{16}$ hydrogen peak at 4.95 ppm is in a clear spectral window and was integrated over the time course of the experiment. Shown in Figure 3 is the absolute integration of the glyoxylate peak in the ^1H NMR spectrum over 23.7 h after the addition of 5 μM ICL. After the addition of ICL to the equilibrium mixture, the concentration of glyoxylate decreases rapidly because of the higher rate of protiated succinate and glyoxylate condensation to form isocitrate relative to the rate of the isocitrate cleavage reaction, which is slowed in D_2O by the solvent KIE. After this initial decrease, the glyoxylate concentration then increases and eventually reaches the new isotopic equilibrium that is experimentally indistinguishable from the original (Figure 3). Because two solvent-derived

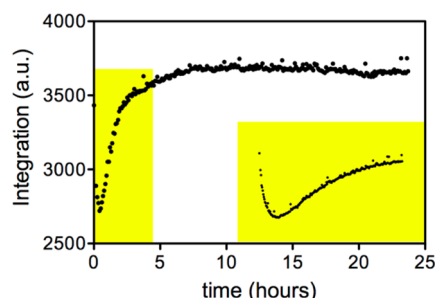


Figure 3. Equilibrium perturbation of glyoxylate. The main panel shows continuous NMR monitoring after the addition of 5 μ M ICL. The inset shows monitoring of the addition of 1 μ M ICL.

protons are incorporated into the C2 and C3 sp^3 C–H bonds in succinate and one is incorporated into the C4 sp^3 C–H bond of isocitrate, the solvent equilibrium effect is predicted to be 0.98 or close to one.¹²

To observe and examine more closely the spectral changes due to the incorporation of deuterium into succinate, we performed an additional equilibrium perturbation experiment at 1 μ M ICL (Figure 4A). The magnitude of the initial peak at 2.32 ppm, corresponding to all protiated succinate decreases with the formation of a peak at 2.31 ppm that transiently increases, then decreases. A peak at 2.30 ppm slowly appears thereafter, representing the final product, dideuterated succinate. The shift in peak resonances is due to the incorporation of deuterium, and we tentatively assign the middle peak to monodeuterated succinate, produced from cleavage of isocitrate in D_2O . We integrated each peak over the course of a similar experiment performed with 5 μ M ICL (Figure 4B). It was not possible to clearly integrate the peaks corresponding to the all protiated isocitrate and monodeuterated isocitrate due to peak overlap (Figure 2).

In the original report about the phenomenon of isotopically induced perturbations to the equilibrium by Schimerlik et al.,¹¹ the ability to observe the perturbation, and its size, was shown to depend on, and be useful in determining, the magnitude of the kinetic isotope effect. In that original treatment, only the situation in which one reactant in an equilibrium mixture was isotopically labeled and transferred to a product without exchange of labeled solvent into, or washout of label from, either reactant was examined. Clearly, that is not the situation with isocitrate lyase, where both products and reactants exchange with solvent isotope, and in the case of succinate,

multiple times. However, in the original treatment, it was shown that the magnitude of the perturbation could be correlated with the kinetic isotope effect. Isotope effects determined by the equilibrium perturbation method, termed $^D(\text{Eq.Pert.})$, are most similar to the corresponding $^DV/K$ effects. Although we probed the perturbation with a substrate that does not become isotopically labeled, we have used it as a surrogate for the solvent kinetic isotope effect on isocitrate cleavage, because this is where the solvent isotope is incorporated into the first formed product, monodeuterosuccinate (Scheme 1). Using eq 2 from the original reference¹¹

$$[R_{\text{max}}] - [R_0]/[R'_0] = \alpha^{-1/(\alpha-1)} - \alpha^{-\alpha/(\alpha-1)} \quad (2)$$

where $[R_{\text{max}}] - [R_0]/[R'_0]$ represents the relative magnitude of the equilibrium perturbation and α represents the estimated kinetic isotope effect on V/K , we calculate a displacement of 0.259, which corresponds to an isotope effect of 2.0–2.1. This can be compared to the experimentally determined $^D_2\text{O}[V/K_{\text{isocitrate}}]$ value in the steady state of 2.2 ± 0.3 .

Mass Spectrometry. Using mass spectrometry, we examined the conversions of isocitrate to monodeuterated isocitrate and succinate to mono- and dideuterated succinate from the point of ICL addition until the return to equilibrium (Figure 5). Immediately following the additions of ICL, we observe a decrease in the amount of protiated isocitrate and an increase in the amount of monodeuterated isocitrate (Figure 5A). This continues until all the isocitrate in the reaction is present in the monodeuterated form. We can also observe a slight equilibrium perturbation at the first three points where the isocitrate concentration briefly increases before the more marked decrease. This confirms our results observed with glyoxylate (Figure 3). If the glyoxylate concentration initially decreases, the isocitrate concentration must initially increase. For succinate, we see a rapid decrease in the concentration of the protiated species that is accompanied by an increase in the concentration of the monodeuterated species and a slower increase in the concentration of the dideuterated species (Figure 5B). After approximately 2 h, the concentration of the monodeuterated succinate peaks begins to decrease, and eventually, all the succinate is dideuterated. This pattern of formation and depletion of each of the succinate species confirms what we found when the reaction was monitored by ^1H NMR spectroscopy (Figure 4B). These data could be fit to equations describing single-exponential behavior, and rate

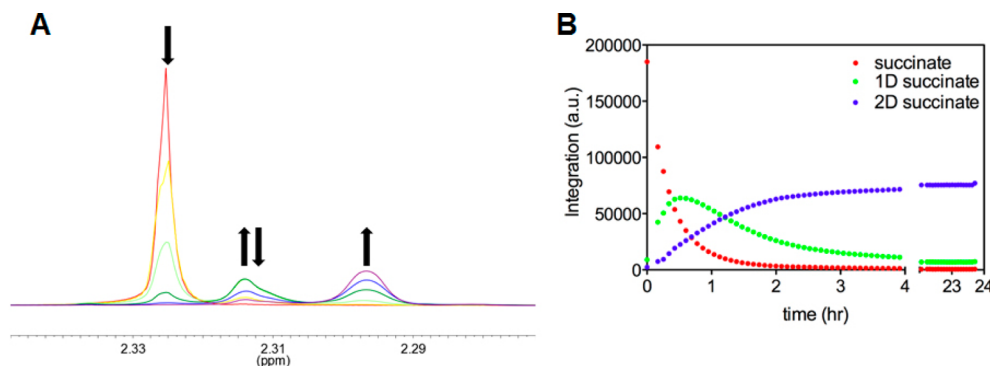


Figure 4. Time course of succinate ^1H resonances. (A) The red scan was taken before 1 μ M ICL was added, the yellow scan 10 min after the addition of ICL, the light green scan after 104 min, the dark green scan after 329 min, the blue scan after 659 min, and the purple scan after 1313 min. (B) Integration of each isotopic form of succinate after the addition of 5 μ M ICL over 23.7 h. Time zero is before ICL addition.

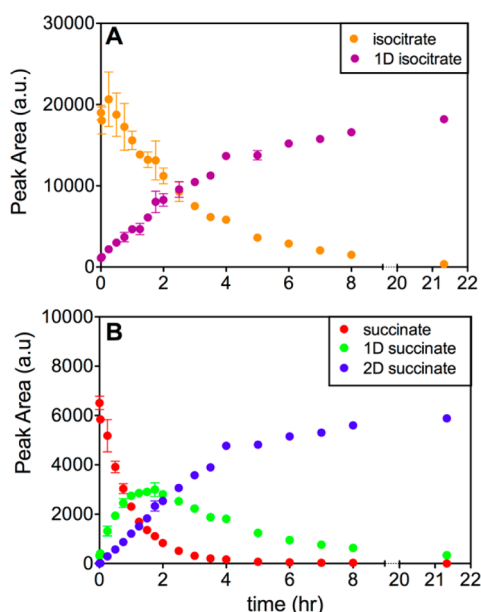


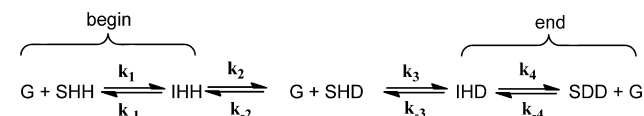
Figure 5. Change in isotopic composition over time determined by mass spectrometry. (A) Conversion of isocitrate to monodeuterated isocitrate. (B) Conversion of succinate to dideuterated succinate through a transient monodeuterated succinate species.

constants from the formation of each species were determined (Figure 6).

Modeling and Simulation. With these data in hand, we queried whether we could generate a model and set of rate

constants that could qualitatively simulate the mass spectrometric data for the time course for the appearance and disappearance of the various isotopic species. We used a chemically reasonable model shown in Scheme 2 corresponding

Scheme 2. Model for the Equilibrium Perturbation of the ICL-Catalyzed Reaction by D_2O^a



^aAbbreviations: SHH, fully protiated succinate; G, glyoxylate; IHH, fully protiated isocitrate; SHD, monodeuterated succinate; IHD, monodeuterated isocitrate; SDD, dideuterated succinate.

to the isotopologues identified in Scheme 1, where the identities of the isotopic species of isocitrate and succinate are noted. Initial estimates for the rates of all protio-succinate disappearance were obtained by fitting the mass spectrometric data to a single exponential. All calculated rate constants were in the range of $0.7\text{--}3.0 \times 10^{-4} \text{ s}^{-1}$. There are several simulation constraints in the model. The rate constant for conversion of isocitrate to glyoxylate and monodeuterated succinate, k_2 , should be similar to the rate constant for conversion of monodeuterated isocitrate to glyoxylate and dideuterated succinate, k_4 , perhaps with a very small difference that is a result of a secondary kinetic isotope effect. Similarly, the rate constant for conversion of monodeuterated succinate to protio-isocitrate, k_{-2} , should be similar to the rate constant for conversion of dideuterated succinate to monodeuterated

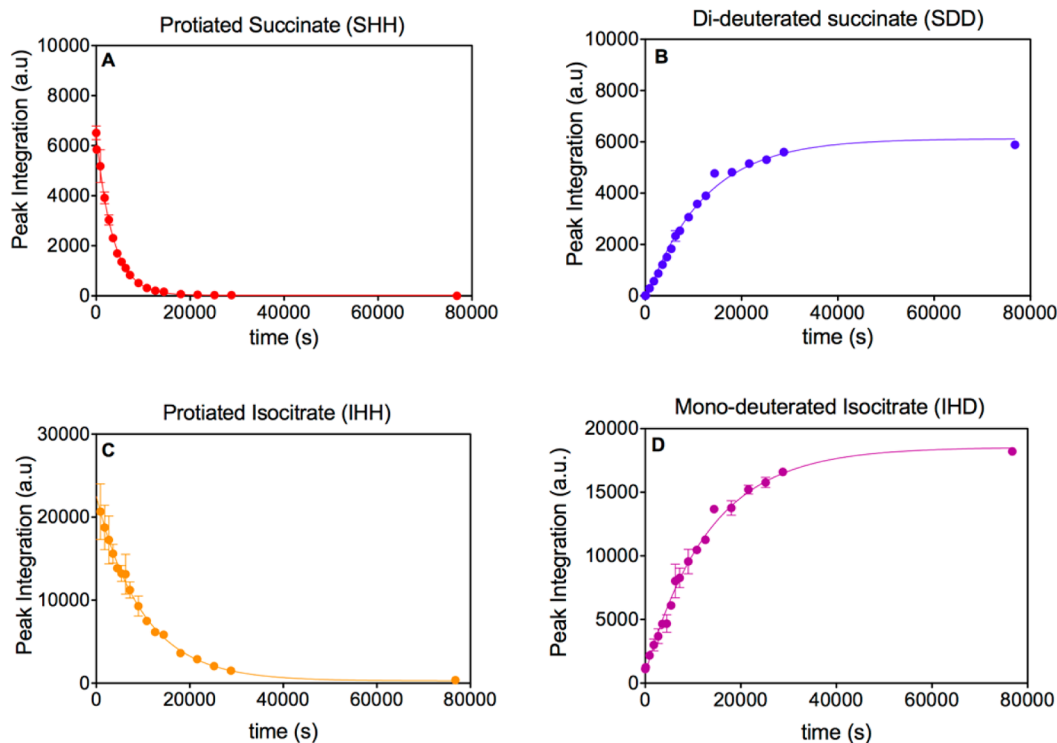


Figure 6. Determination of rate constants from the mass spectrometric data. (A) The decrease in the concentration of SHH was fit to the equation $y = (y_0 - a)e^{-kt} + a$, yielding a k of $2.81 \times 10^{-4} \pm 8 \times 10^{-6} \text{ s}^{-1}$. (B) The increase in the concentration of SDD was fit to the equation $y = y_0 + (a - y_0)(1 - e^{-kt})$, yielding a k of $8.4 \times 10^{-5} \pm 3 \times 10^{-6} \text{ s}^{-1}$. (C) The decrease in the concentration of IHH was fit to the equation $(y = y_0 - a)e^{(-kt)} + a)$ (the first two time points were excluded from this fit), yielding a k of $1.01 \times 10^{-4} \pm 8 \times 10^{-6} \text{ s}^{-1}$. (D) The increase in the concentration of IHD was fit to the equation $y = y_0 + (a - y_0)(1 - e^{-kt})$, yielding a k of $7.5 \times 10^{-5} \pm 3 \times 10^{-6} \text{ s}^{-1}$.

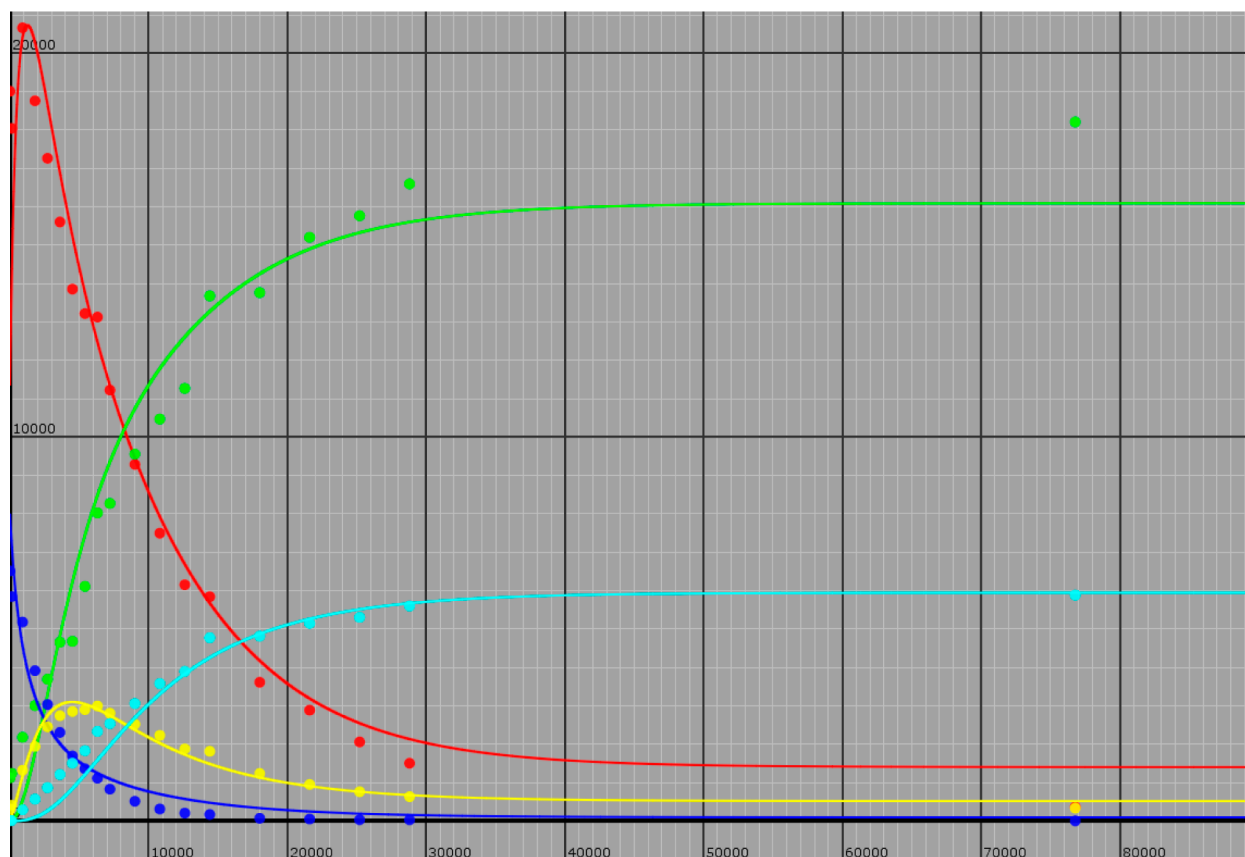


Figure 7. Global simulation of mass spectrometry data. The model shown in Scheme 2 was used as was KinTek Global Kinetic Explorer (version 3.0.2362). Isotopic species are all protio-isocitrate (red), all protio-succinate (blue), monodeuteroisocitrate (green), monodeuterated succinate (yellow), and dideuterosuccinate (light blue). The rate constants yielding the curves through the experimental points are as follows: $k_1 = 9.53 \times 10^{-5} \text{ s}^{-1}$, $k_{-1} = 2.33 \times 10^{-4} \text{ s}^{-1}$, $k_2 = 3.83 \times 10^{-4} \text{ s}^{-1}$, $k_{-2} = 2.83 \times 10^{-4} \text{ s}^{-1}$, $k_3 = 3.43 \times 10^{-5} \text{ s}^{-1}$, $k_{-3} = 4.05 \times 10^{-5} \text{ s}^{-1}$, $k_4 = 3.83 \times 10^{-5} \text{ s}^{-1}$, and $k_{-4} = 2.83 \times 10^{-4} \text{ s}^{-1}$.

isocitrate, k_{-4} , again with a possible small difference due to a secondary kinetic isotope effect. These two sets of rate constants were held equal during the simulation.¹⁷

As seen in Figure 7, reasonable values for all eight rate constants could be obtained, which qualitatively fit the time course of the appearance and disappearance for all isotopically labeled substrates and products. This includes an initial increase in the protio-isocitrate concentration due to the equilibrium perturbation, which is equal and opposite to that observed for glyoxylate (Figure 3), and the predicted increase and then decrease in monodeuterated succinate concentration as it is initially formed in D_2O from isocitrate cleavage and then ultimately converted into dideuterated succinate from cleavage of deuterated isocitrate. The largest deviations are observed when the concentrations of species are small, and this is likely due to the larger errors in the measurement of the absolute amounts of these species by mass spectrometry. Finally, although the reverse fluxes of species via steps with associated rate constants k_{-1} and k_{-3} are likely to be small, the data could not be easily fit when these rate constants were set to zero.

CONCLUSIONS

In this study, we report the solvent isotope-induced transient change in the concentration and isotopic composition of the reactants. These effects were determined using a combination of ^1H NMR spectroscopy and mass spectrometry, because no absorbance changes are manifest during the reaction. The

normal solvent kinetic isotope effect for isocitrate cleavage generated an equilibrium perturbation whose size and direction were predicted by the solvent kinetic isotope effect. Mass spectrometry of the reactants as a function of time revealed the incorporation of solvent-derived deuterium into isocitrate and succinate; the initial formation of monodeuterosuccinate was followed by the eventual formation of dideuterosuccinate. A chemically reasonable model was generated, and rate constants that could qualitatively simulate the experimental results were obtained.

Isocitrate lyase catalyzes the cleavage of isocitrate in D_2O to form monodeuterosuccinate, a symmetric molecule that is asymmetrically isotopically labeled. This aspect of the reaction is similar to that of the reaction of diaminopimelate (DAP) epimerase, in which D,L-DAP is converted into monodeutero- L,L-DAP , which is similarly a symmetric molecule with asymmetric isotope labeling. This results in a double overshoot for which a mechanism was proposed and modeled.¹⁸ We report here the first determination of a solvent kinetic isotope effect-induced equilibrium perturbation by ^1H NMR spectroscopy. The idea was suggested by the large steady-state solvent kinetic isotope effect on isocitrate cleavage, performed by NMR spectroscopy because of the lack of any spectroscopic change associated with the reaction and confirmed by mass spectrometry. Further investigation is required to determine whether this method can be used to quantitatively determine the kinetic isotope effect in the isocitrate lyase system; however,

there are a large number of non-redox enzyme-catalyzed chemistries, including the large class of aldol and Claisen-type cleavage reactions and isomerases, for which this method may be broadly applicable for estimating kinetic isotope effects. The widespread availability and stability of modern NMR instruments and mass spectrometers should make its implementation routine.

AUTHOR INFORMATION

Corresponding Author

*Department of Biochemistry, Albert Einstein College of Medicine, 1300 Morris Park Ave., Bronx, NY 10461. E-mail: john.blanchard@einstein.yu.edu. Phone: (718) 430-3096. Fax: (718) 430-8565.

Funding

This work was supported by National Institutes of Health Grant AI60899 to J.S.B. The instrumentation in the Structural NMR Resource is supported by the Albert Einstein College of Medicine.

Notes

The authors declare no competing financial interest.

ACKNOWLEDGMENTS

We thank Dr. William R. Jacobs, Jr., for allowing us to use his mass spectrometer for the equilibrium perturbation experiments and Drs. Brian Weinrick and Travis Hartman for training and insightful discussions. We thank Dr. Hui Xiao for performing the initial mass spectrometric identification of the deuterated species and Dr. Syun-Ru Yeh and Dr. Ariel Lewis for use and instruction on their circular dichroism machine. We thank Mary Thompson for performing the purification of ICL and efforts in initial assay development.

DEDICATION

This work is dedicated to the memory of W. W. Cleland.

ADDITIONAL NOTE

^aThe Haldane relationship represents the equality of the equilibrium constant and the kinetic parameters for the reaction catalyzed. For the isocitrate lyase reaction that exhibits a uni-bi kinetic mechanism (isocitrate > glyoxylate + succinate), the relevant Haldane relationship¹⁹ is $K_{eq} = (V_1 K_{ip} K_q) / (V_2 K_{ia})$, where V_1 and V_2 are the maximal velocities in the isocitrate cleavage reaction and the aldol condensation reaction, respectively. There is strong evidence of the binding of glyoxylate to the active site metal ion prior to succinate binding, and therefore, K_{ia} is the dissociation constant for isocitrate, K_{ip} the dissociation constant for succinate, and K_q the Michaelis constant for glyoxylate. Assuming that the determined Michaelis constants for isocitrate and succinate are reasonable approximations of the dissociation constants, our experimentally determined kinetic constants (see Results and Discussion) can be used to calculate an equilibrium constant of 0.0003. This is within a factor of 3.5 of the experimentally determined value of 0.0011, which considering the standard errors for the determined kinetic parameters and the assumption that the Michaelis and dissociation constants for the substrates are similar is in good agreement. It also suggests that glyoxylate hydration or dehydration is fast, because the total concentration of glyoxylate was used in the calculation of K_{eq} .

REFERENCES

- (1) Kondrashov, F. A., Koonin, E. V., Morgunov, I. G., Finogenova, T. V., and Kondrashova, M. N. (2006) Evolution of glyoxylate cycle enzymes in Metazoa: Evidence of multiple horizontal transfer events and pseudogene formation. *Biol. Direct* 1, 31.
- (2) McKinney, J. D., Honer zu Bentrup, K., Munoz-Elias, E. J., Miczak, A., Chen, B., Chan, W. T., Swenson, D., Sacchettini, J. C., Jacobs, W. R., Jr., and Russell, D. G. (2000) Persistence of *Mycobacterium tuberculosis* in macrophages and mice requires the glyoxylate shunt enzyme isocitrate lyase. *Nature* 406, 735–738.
- (3) Campbell, J. J., Smith, R. A., and Eagles, B. A. (1953) A deviation from the conventional tricarboxylic acid cycle in *Pseudomonas aeruginosa*. *Biochim. Biophys. Acta* 11, 594.
- (4) Smith, R. A., and Gunsalus, I. C. (1954) Isocitritase: A New Tricarboxylic Acid Cleavage System. *J. Am. Chem. Soc.* 76, 5002–5003.
- (5) Smith, R. A., and Gunsalus, I. C. (1955) Distribution and formation of isocitritase. *Nature* 175, 774–775.
- (6) Smith, R. A., and Gunsalus, I. C. (1957) Isocitritase; enzyme properties and reaction equilibrium. *J. Biol. Chem.* 229, 305–319.
- (7) Sprecher, M., Berger, R., and Sprinson, D. B. (1964) Stereochemistry of the isocitrate lyase reaction. *Biochem. Biophys. Res. Commun.* 16, 254–257.
- (8) Sprecher, M., Berger, R., and Sprinson, D. B. (1964) Stereochemical Course of the Isocitrate Lyase Reaction. *J. Biol. Chem.* 239, 4268–4271.
- (9) Sharma, V., Sharma, S., Hoener zu Bentrup, K., McKinney, J. D., Russell, D. G., Jacobs, W. R., Jr., and Sacchettini, J. C. (2000) Structure of isocitrate lyase, a persistence factor of *Mycobacterium tuberculosis*. *Nat. Struct. Biol.* 7, 663–668.
- (10) Cardinale, G. J., and Abeles, R. H. (1968) Purification and mechanism of action of proline racemase. *Biochemistry* 7, 3970–3978.
- (11) Schimerlik, M. I., Rife, J. E., and Cleland, W. W. (1975) Equilibrium perturbation by isotope substitution. *Biochemistry* 14, 5347–5354.
- (12) Blanchard, J. S., and Cleland, W. W. (1980) Use of isotope effects to deduce the chemical mechanism of fumarase. *Biochemistry* 19, 4506–4513.
- (13) Quartararo, C. E., Hazra, S., Hadi, T., and Blanchard, J. S. (2013) Structural, Kinetic and Chemical Mechanism of Isocitrate Dehydrogenase-1 from *Mycobacterium tuberculosis*. *Biochemistry* 52, 1765–1775.
- (14) ExPASy (2011) ProtParam Tool (<http://ca.expasy.org/tools/protparam.html>) (accessed June 15, 2011).
- (15) Moynihan, M. M., and Murkin, A. S. (2013) personal communication.
- (16) Meany, J. E., and Pocker, Y. (1991) The Dehydration of Glyoxylate Hydrate: General-Acid, General-Base, Metal Ion, and Enzymatic Catalysis. *J. Am. Chem. Soc.* 113, 6155–6161.
- (17) Johnson, K. A., Simpson, Z. B., and Blom, T. (2009) Global kinetic explorer: a new computer program for dynamic simulation and fitting of kinetic data. *Anal. Biochemistry* 387, 20–29.
- (18) Koo, C. W., and Blanchard, J. S. (1999) The Chemical Mechanism of *Haemophilus influenzae* Diaminopimelate Epimerase. *Biochemistry* 38, 4416–4422.
- (19) Cleland, W. W. (1982) An Analysis of Haldane Relationships. *Methods Enzymol.* 87, 366–369.